The T-Box transcription factor Tbx5 is required for the patterning and maturation of the murine cardiac conduction system

Ivan P. G. Moskowitz[1,2], Anne Pizard[1,9], Vickas V. Patel[3,4], Benoit G. Bruneau[5,6], Jae B. Kim[1], Sabina Kupershmidt[7], Dan Roden[8], Charles I. Berul[4], Christine E. Seidman[1,9] and Jonathan G. Seidman[1,*]

[1]Department of Genetics, Harvard Medical School and Howard Hughes Medical Institute, Boston, MA 02115, USA
[2]Department of Pathology and Cardiac Registry, Children's Hospital and Harvard Medical School, Boston, MA 02115, USA
[3]Molecular Cardiology Research Center and Section of Cardiac Electrophysiology, University of Pennsylvania, Philadelphia, PA 19104, USA
[4]Department of Cardiology, Children's Hospital and Department of Pediatrics, Harvard Medical School, Boston, MA 02115, USA
[5]Programs in Cardiovascular Research and Developmental Biology, The Hospital for Sick Children, Toronto, ON M5G 1X8, Canada
[6]Department of Molecular and Medical Genetics, University of Toronto, Toronto, ON M5S 1A8, Canada
[7]Departments of Anesthesiology and Pharmacology, Vanderbilt University School of Medicine, Nashville, TN 37232-6602, USA
[8]Departments of Medicine and Pharmacology, Vanderbilt University School of Medicine, Nashville, TN 37232-6602, USA
[9]Division of Cardiology, Brigham and Women's Hospital, and Howard Hughes Medical Institute, Boston, MA 02115,USA
*Author for correspondence (e-mail: seidman@genetics.med.Harvard.edu)

Accepted 4 May 2004

Development 131, 4107-4116
Published by The Company of Biologists 2004
doi:10.1242/dev.01265

Summary

We report a critical role for the T-box transcription factor Tbx5 in development and maturation of the cardiac conduction system. We find that *Tbx5* is expressed throughout the central conduction system, including the atrioventricular bundle and bundle branch conduction system. *Tbx5* haploinsufficiency in mice (*Tbx5*$^{del/+}$), a model of human Holt–Oram syndrome, caused distinct morphological and functional defects in the atrioventricular and bundle branch conduction systems. In the atrioventricular canal, *Tbx5* haploinsufficiency caused a maturation failure of conduction system morphology and function. Electrophysiologic testing of *Tbx5*$^{del/+}$ mice suggested a specific atrioventricular node maturation failure. In the ventricular conduction system, *Tbx5* haploinsufficiency caused patterning defects of both the left and right ventricular bundle branches, including absence or severe abnormalities of the right bundle branch. Absence of the right bundle branch correlated with right-bundle-branch block by ECG. Deficiencies in the gap junction protein gene connexin 40 (*Cx40*), a downstream target of *Tbx5*, did not account for morphologic conduction system defects in *Tbx5*$^{del/+}$ mice. We conclude that *Tbx5* is required for *Cx40*-independent patterning of the cardiac conduction system, and suggest that the electrophysiologic defects in Holt–Oram syndrome reflect a developmental abnormality of the conduction system.

Key words: Cardiac, Conduction, Tbx5, Mouse

Introduction

The cardiac conduction system comprises a specialized subset of myocardial cells essential for the coordinated contraction of the multi-chambered vertebrate heart. Composed of the sinoatrial node, atrioventricular node, atrioventricular bundle and ventricular bundle branches, the central cardiac conduction system and associated peripheral Purkinje fibers have distinct electrophysiological, morphological and transcriptional profiles from the surrounding working myocardium (reviewed by Moorman et al., 1998; Gourdie et al., 2003). While some genes involved in the biologic functions of the mature conduction system have been identified, few genes required for the pattern formation of the evolutionarily conserved structure of the vertebrate cardiac conduction system, or for the differentiation of the specialized cells that comprise the conduction system, are known (Nguyen-Tran et al., 2000) (reviewed by Cheng et al., 2003).

A molecular marker of the conduction system has been reported, in a study in which selective β-galactosidase expression in the cardiac conduction system was established by placing the *lacZ* gene downstream of the potassium channel *minK* promoter (Kupershmidt et al., 1999; Kondo et al., 2003). In adult mice, β-galactosidase expression from the *minK:lacZ* allele (*minK*$^{lacZ/+}$) demarcates nuclei of cells in the mature central conduction system, including the sinoatrial node, the atrioventricular node, the atrioventricular bundle and the right and left bundle branches, from the working myocardium. In concert with in-vivo electrophysiologic techniques (Gehrmann and Berul, 2000), *minK*$^{lacZ/+}$ mice enable detailed morphological and functional analyses of the mammalian conduction system.

We employed these tools to study the role of the transcription factor Tbx5 in the development of the cardiac conduction system. *Tbx5* belongs to the T-box gene family, the members of which share a highly conserved 180-amino-acid domain required for DNA binding (Herrmann et al.,

1990; Muller and Herrmann 1997) (reviewed by Papaioannou and Silver, 1998). Mutations in several human T-box genes cause dominant disorders with a variety of developmental malformations (Bamshad et al., 1997; Merscher et al., 2001). In humans, haploinsufficiency of functionally null *TBX5* mutations causes Holt–Oram syndrome (Basson et al., 1997; Li et al., 1997; Basson et al., 1999), manifest by congenital heart defects, conduction-system abnormalities and upper-limb deformities. Morphologic cardiac defects are most commonly atrial septal defects of the secundum type, although a range of structural abnormalities has been reported (Basson et al., 1997; Li et al., 1997, Basson et al., 1999). Common electrophysiologic abnormalities found in Holt–Oram syndrome include progressive atrioventricular block, bundle-branch block and sick sinus syndrome (Basson et al., 1994). Some Holt–Oram syndrome patients have electrophysiologic defects in the absence of structural heart defects (Basson et al., 1994; Newbury-Ecob et al., 1996), thereby suggesting a direct role for *TBX5* in the conduction system that is independent of this transcription factor's function in cardiac septation.

Mice lacking a functional *Tbx5* allele (*Tbx5*$^{del/+}$) were constructed to understand how *Tbx5* haploinsufficiency disturbs limb and cardiac development (Bruneau et al., 2001). Like Holt–Oram patients, adult *Tbx5*$^{del/+}$ mice were found to have atrial septal defects (ASDs), including secundum or primum ASDs, and conduction system abnormalities including atrioventricular conduction delay. Molecular studies of *Tbx5*$^{del/+}$ mice identified *atrial natriuretic factor* (*ANF*) and connexin 40 (*Cx40*; *Gja5* – Mouse Genome Informatics) as gene targets of this transcription factor: expression of *ANF* and *Cx40* is abrogated in *Tbx5*$^{del/+}$ mice. Both *ANF* and *Cx40* are expressed in cells of the conduction system (Houweling et al., 2002; Coppen et al., 2003). Cx40 is localized at cellular appositions called gap junctions, which function to propagate electrical impulses between cells. *Cx40* null mice (*Cx40*$^{-/-}$) have electrophysiologic defects similar to *Tbx5*$^{del/+}$ mice, including atrioventricular block and bundle-branch block. Taken together, previous work suggested that *Cx40* deficiency could account for conduction system disease in *Tbx5*$^{del/+}$ mice and in Holt–Oram syndrome.

To study the role of *Tbx5* in conduction system development, we examined the expression of this transcription factor during the anatomical and functional maturation of the cardiac electrophysiologic system. We investigated the consequences of *Tbx5* haploinsufficiency on central conduction system function and morphology by analyzing wild-type, *Tbx5*$^{del/+}$ and compound *Tbx5*$^{del/+}$/*minK*$^{lacZ/+}$ mice and *Cx40*$^{-/-}$/*minK*$^{lacZ/+}$ mice. We report specific developmental and functional requirements for *Tbx5* in the atrioventricular node, atrioventricular (His) bundle and bundle branches of the conduction system. These findings identify *Tbx5* as a critical transcription factor for the morphologic patterning and electrophysiologic maturation of the mammalian conduction system.

Materials and methods

Animals

Creation of *Tbx5* and *Cx40* knockout mice has been previously described (Simon et al., 1998; Bruneau et al., 2001). All mice were analyzed as 129 SV inbred. All protocols conformed to the Association for the Assessment and Accreditation of Laboratory Animal Care and the Children's Hospital Animal Care and Use Committee.

ECGs

Surface ECGs were recorded from unanesthetized *Tbx5*$^{del/+}$ newborn mice (n=14) and compared with those for littermate wild-type mice (n=22). Surface ECG recordings and complete in-vivo electrophysiological studies (EPS) were recorded from 14-week-old adult *Tbx5*$^{del/+}$ mice (n=21) and compared with those for wild-type littermate mice (n=13). Surface ECG recordings were also recorded from 14-week-old adult *Cx40*$^{-/-}$/*minK*$^{lacZ/+}$ and *Tbx5*$^{del/+}$/*minK*$^{lacZ/+}$ mice (n=19) and compared with those for age-matched wild-type mice (n=14).

Protocols for the surface ECG and in-vivo mouse electrophysiology studies are previously described (Berul et al., 1996; Maguire et al., 2000). Briefly, 6-limb ECGs with a right precordial lead were obtained using 25-gauge subcutaneous electrodes in unanesthetized newborn mice. Adult mice were lightly anesthetized with pentobarbital (0.033 mg/kg IP) and 6-limb lead ECGs with a right precordial lead were obtained using 25-gauge subcutaneous electrodes. For in-vivo electrophysiology studies in adult mice, a jugular vein cutdown was performed and an octapolar 2-French electrode catheter (CIBer mouse-EP; NuMED, Inc.) was placed in the right atrium and ventricle under electrogram guidance to confirm catheter position. Recording of atrioventricular bundle potentials was confirmed by the presence of a triphasic signal on one of the distal bipole electrograms, and was accomplished using simultaneous multielectrodes and persistent catheter manipulation (Maguire et al., 2000).

Electrophysiology study

In-vivo electrophysiologic studies were performed in all adult mice using standard pacing protocols to assess atrial and ventricular conduction, refractoriness and arrhythmia inducibility (Maguire et al., 2000; Berul et al., 2001). ECG channels were filtered between 0.5 and 250 Hz and intracardiac electrograms filtered between 5 and 400 Hz. Signals were displayed on an oscilloscope and simultaneously recorded through an A-D converter at a digitization rate of 2 kHz (MacLab Systems, Inc.) for offline analysis. ECG intervals were measured in 6-limb leads and a right precordial lead by two independent observers, blinded to genotype.

β-galactosidase (*lacZ*) activity

Dissected hearts were fixed at 4°C in 4% paraformaldehyde in 0.1 mol/L PBS (pH 7.4) for 1 hour. Following a PBS rinse, hearts were permeabilized in 0.01% sodium deoxycholate, 0.02% NP-40, and 2 mmol/L $MgCl_2$ in 0.1 mol/L PBS for 30 minutes. Following a PBS rinse, hearts were stained in permeabilization solution plus 1 mg/ml X-Gal, 5 mmol/L potassium ferrocyanide, and 5 mmol/L ferrocyanide at 37°C overnight. Hearts were washed at least three times with PBS and post-fixed and stored in 4% paraformaldehyde at 4°C.

In-situ hybridization

Whole-mount in-situ hybridization was performed as previously described (Bruneau et al., 2001). To insure probe access to the entire heart, the systemic and pulmonary veins were opened and the ventricular apex was removed. In-situ hybridization was performed on slide sections with the following modifications. Newborn hearts were dissected, washed once in PBS, fixed overnight in 4% paraformaldehyde in PBS and either stored at room temperature in ethanol 70% or immediately paraffin embedded and sectioned. In-situ hybridization on paraffin wax tissue sectioned at 5 μm was performed using radioactive *Tbx5* probe (Bruneau et al., 2001) labeled with ^{35}S-UTP according to previously described protocol (Sibony et al., 1995).

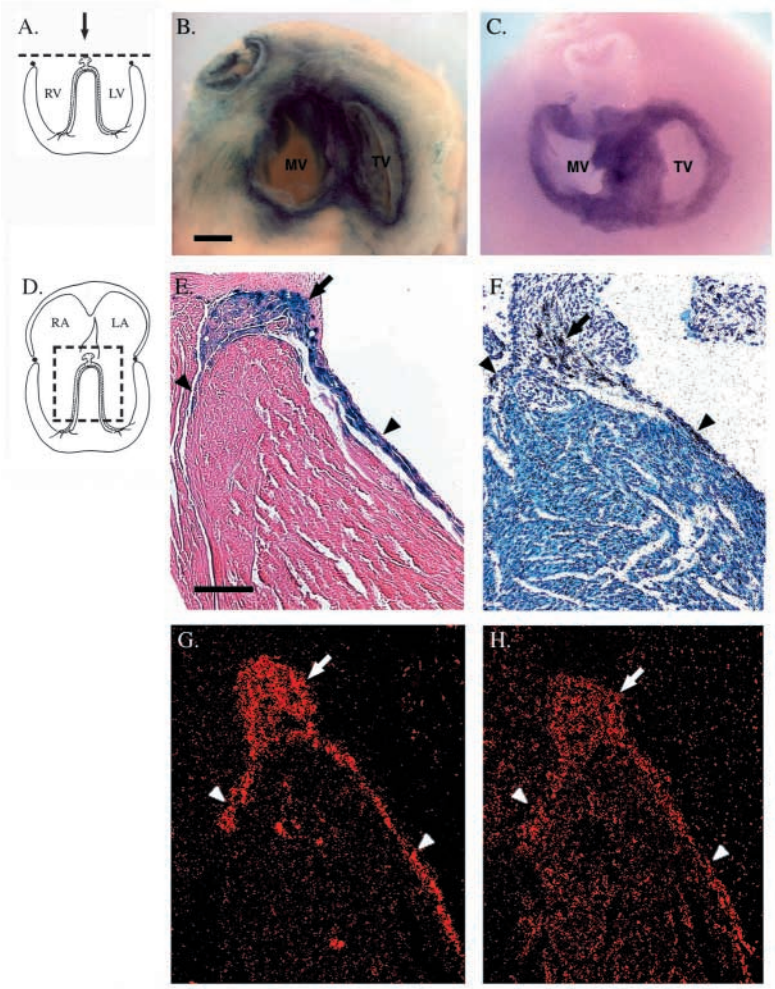

Fig. 1. *Tbx5* is expressed in the murine cardiac conduction system. (A) Schematic representation of the atrioventricular canal conduction system, showing the plane of dissection (dashed line) and specimen orientation (arrow) for images in (B,C). Atria were removed and the atrioventricular canal was viewed from the superior/posterior. The atrioventricular canal from newborn *minK*$^{lacZ/+}$ (B) and wild-type (C) mouse hearts. X-gal staining of *minK*$^{lacZ/+}$ hearts (B) showed two rings of specialized conduction cells, surrounding the tricuspid and mitral annulus. Scale bar: 200 μm. Whole-mount in-situ hybridization with a *Tbx5* probe of wild-type hearts (C) demonstrated rings of *Tbx5* expression that overlap *minK* expression. (D) Schematic representation of dissection of the interventricular septum for images in (E-H). Sagital sections of the muscular interventricular septum of newborn *minK*$^{lacZ/+}$ (E) and wild-type (F-H) mouse hearts. A *minK*$^{lacZ/+}$ heart (E) revealed β-galactosidase activity in the atrioventricular bundle (arrow), and the ventricular bundle branches (arrowheads). Scale bar: 100 μm. In-situ hybridization with a *Tbx5* probe in wild-type hearts (F) demonstrated expression in the atrioventricular bundle (arrow) and bundle branch (arrowheads) conduction system. In-situ hybridization with a connexin 40 probe (G) and *Tbx5* probe (H) in sequential sections from the same wild-type heart demonstrates overlapping expression in the atrioventricular bundle (arrow) and bundle branch (arrowheads) conduction system.

Results

Tbx5 is expressed in the developing cardiac conduction system

The murine conduction system was visualized in mice heterozygous for the *mink:lacZ* allele (*minK*$^{lacZ/+}$) after staining cardiac tissue with X-gal to detect β-galactosidase activity (Fig. 1A,B). Heterozygous *minK*$^{lacZ/+}$ mice have no morphologic or physiologic abnormalities (Kuperschmidt et al., 1999) and β-galactosidase activity demarcates cells of the mature and developing conduction system. The atrioventricular junction was directly viewed after removing both atria (Fig. 1B) and two rings of staining were observed, one surrounding the tricuspid annulus and the other surrounding the mitral annulus. This circumferential pattern is consistent with classic histological and more recent molecular descriptions of the developing atrioventricular conduction system in the vertebrate heart (Wenink 1976; Wessels et al., 1992; Coppen et al., 1999; Davis et al., 2001).

Tbx5 expression was assessed by whole-mount in-situ hybridization in wild-type mouse hearts. Previous work demonstrating high levels of *Tbx5* expression in both atria and the left ventricle and low levels in the right ventricle was confirmed (data not shown) (Bruneau et al., 1999; Hatcher et al., 2000). Abundant *Tbx5* expression was also observed in rings surrounding both the tricuspid annulus and mitral annulus in the atrioventricular canal (Fig. 1C). *Tbx5* expression appeared to co-localize with *minK* expression in both these rings (cf. Fig. 1B,C). No expression was apparent in the atrioventricular valves.

To clarify the relationship between conduction and *Tbx5*-expressing cells, *Tbx5* expression was examined at higher resolution in histologic sections. The conduction system was identified by visualizing β-galactosidase activity in sections from *minK*$^{lacZ/+}$ mouse hearts (Fig. 1E) or connexin 40 expression in sections from wild-type mouse hearts (Fig. 1G). Connexin 40 expression was comparable to that previously described (Coppen et al., 2003). In newborn *minK*$^{lacZ/+}$ mouse hearts, β-galactosidase activity was present in the atrioventricular bundle (Fig. 1E, arrow) and bundle branch (arrowhead) conduction. *Tbx5* expression was observed in the same structures of the centralized conduction system, including the atrioventricular bundle in cross sections from wild-type hearts (Fig. 1F, arrow), and bundle branches (Fig. 1F, arrowheads). Connexin 40 and *Tbx5* expression were assessed by in-situ hybridization on serial sections from the same newborn wild-type heart (Fig. 1G,H, arrow). These RNAs were observed in precisely the same locations in the atrioventricular bundle (Fig. 1G,H, arrow), and left bundle branch and right bundle branch (Fig. 1G,H, arrowheads). A higher level of *Tbx5* expression was observed in the structures of the conduction system than in the surrounding myocardium.

Tbx5 haploinsufficiency prevents atrioventricular canal conduction system maturation

Given *Tbx5* expression in the central conduction system of newborn mice and ECG abnormalities in *Tbx5*$^{del/+}$ mice (Bruneau et al., 2001), we hypothesized that *Tbx5* haploinsufficiency might affect conduction system

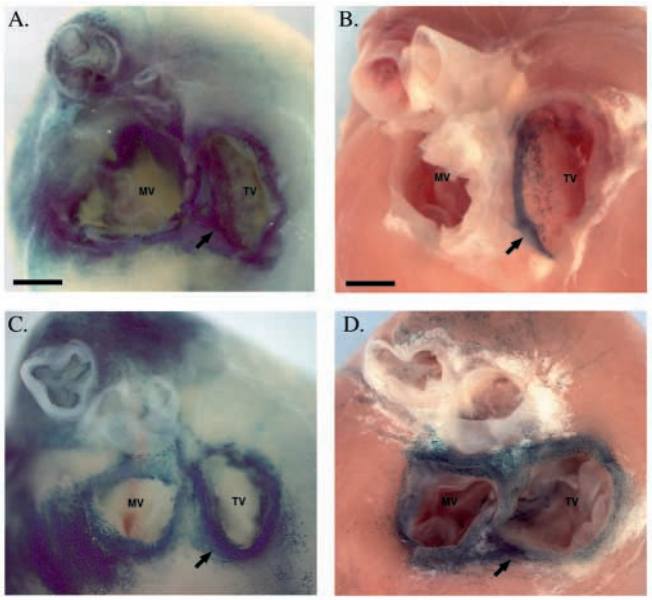

Fig. 2. Conduction system maturation failure in *Tbx5*$^{del/+}$ mice. The atrioventricular canal conduction system in *minK*$^{lacZ/+}$ (A,B) and *Tbx5*$^{del/+}$*/minK*$^{lacZ/+}$ (C,D) hearts was studied in newborn (A,C) and adult (B,D) mice. The atria were removed and the atrioventricular canal was viewed from the superior/posterior, with the tricuspid annulus on the right and the mitral annulus on the left. Rings of specialized conduction cells observed in the atrioventricular canal of newborn *minK*$^{lacZ/+}$ mouse hearts (A) matured into a well-defined atrioventricular node (arrow) and atrioventricular bundle in adult *minK*$^{lacZ/+}$ mouse hearts (B). (A) Scale bar: 200 μm. (B) Scale bar: 800 μm. Rings of specialized conduction cells in the atrioventricular canal of newborn *Tbx5*$^{del/+}$*/minK*$^{lacZ/+}$ mouse hearts (C) failed to mature into a discrete atrioventricular node or atrioventricular bundle in adult *Tbx5*$^{del/+}$*/minK*$^{lacZ/+}$ mouse hearts (D). Instead the neonatal pattern (rings of specialized conduction tissue) was maintained. Arrow denotes expected location of the atrioventricular node.

development. Hearts from compound heterozygous *Tbx5*$^{del/+}$*/minK*$^{lacZ/+}$ mice (see Materials and methods) and *minK*$^{lacZ/+}$ mice were compared after X-gal staining. At the atrioventricular junction, hearts from newborn *minK*$^{lacZ/+}$ (Fig. 2A) and *Tbx5*$^{del/+}$*/minK*$^{lacZ/+}$ (Fig. 2C) mice demonstrated similar rings of specialized conduction tissue surrounding both the tricuspid annulus and mitral annulus. This same pattern of β-galactosidase activity was observed in all *minK*$^{lacZ/+}$ (n=25) and *Tbx5*$^{del/+}$*/minK*$^{lacZ/+}$ (n=22) newborn mouse hearts.

Expression of β-galactosidase in hearts from 14-week-old adult *minK*$^{lacZ/+}$ mice revealed a mature conduction system with a strikingly different structure than that observed in the newborn mouse (cf. Fig. 2A,B). Adult *minK*$^{lacZ/+}$ hearts no longer showed the atrioventricular rings found in newborns but instead exhibited a more restricted expression of β-galactosidase activity consolidated in the atrioventricular node and atrioventricular bundle. The striking morphologic changes in the conduction system between newborn and adult mice indicate that postnatal development of the electrophysiologic system is essential for establishment of the mature structures found in adults. By contrast, adult *Tbx5*$^{del/+}$*/minK*$^{lacZ/+}$ mice (Fig. 2D) did not demonstrate restricted expression of β-galactosidase activity. There was no localized staining of the atrioventricular node and bundle, and instead there was a persistence of β-galactosidase activity in both atrioventricular rings, which remarkably resembled the pattern observed in hearts from newborn mice (Fig. 2C).

Table 1. Conduction intervals from wild-type and *Tbx5*$^{(del/–)}$ mice

A. Electrocardiology*

	Newborn	Adult	*P*-value (newborn:adult)
Wild-type PQ interval	48.0±7.6	41.9±1.0	<0.001
Tbx5$^{(del/+)}$ PQ interval	50.7±5.8	49.1±4.6	<0.46
P-value†	0.38	<0.01	
Wild-type QRS interval	9.8±1.5	13.7±1.3	<0.01
Tbx5$^{(del/+)}$ QRS interval	12.7±2.6	16.5±1.0	<0.01
P-value‡	<0.001	<0.005	

B. Electrophysiology§

	Wild-type adult	*Tbx5*$^{(del/+)}$ adult	*P*-value (wild-type:*Tbx5*$^{(del/+)}$)
AH interval	37.0±1.5	42.3±6.0	<0.001
HV interval	11.5±1.5	10.3±2.0	<0.69
P-wave duration	15.0±1.1	15.9±2.5	<0.36

*PQ and QRS intervals were compared in newborn and adult wild-type and *Tbx5*$^{del/+}$ mice. The PQ interval is not significantly different between newborn *Tbx5*$^{del/+}$ and wild-type mice, but was significantly longer in adult *Tbx5*$^{del/+}$ than in adult wild-type mice. Note that the PQ interval of wild-type mice shortens with age, whereas the PQ interval of *Tbx5*$^{del/+}$ mice fails to undergo physiologic shortening in the postnatal period. The QRS interval is significantly longer in both newborn and adult *Tbx5*$^{del/+}$ mice compared with age-matched wild-type mice.

†Wild-type PQ interval:*Tbx5*$^{(del/+)}$ PQ interval.

‡Wild-type QRS interval:*Tbx5*$^{(del/+)}$ QRS interval.

§The AH and HV interval and *P*-wave duration were compared in adult wild-type and *Tbx5*$^{del/+}$ mice. The HV interval and *P*-wave duration are not significantly different between wild-type and *Tbx5*$^{del/+}$ adult mice. However, the AH interval is significantly longer in *Tbx5*$^{del/+}$ mice than in wild-type adult mice.

To ascertain whether *Tbx5* had functional, as well as morphological, roles in atrioventricular conduction system maturation, we evaluated the consequences of *Tbx5* haploinsufficiency using surface ECG monitoring and in-vivo electrophysiology. Surface ECGs were recorded from un-anesthetized, newborn animals and lightly anesthetized adult animals. The PQ interval, which detects the time for electrical conduction from the sinoatrial node to the atrioventricular node, atrioventricular bundle, and proximal bundle branches, was measured (Fig. 3A, Table 1) (Marriott and Conover, 1998). As previously described (Bruneau et al., 2001), adult *Tbx5*$^{del/+}$ mice have a prolonged PQ interval compared with that of wild-type mice (49.1±4.6 ms vs. 41.9±1.0 ms; P<0.01) (Fig. 3B, Table 1). However, in newborn mice, the PQ intervals of wild-type and *Tbx5*$^{del/+}$ mice were not significantly different (48.0±7.6 ms vs. 50.7±5.8 ms; P<0.38) (Fig. 3B, Table 1). Neither the presence of the *minK*^{lacZ} allele nor the type of atrial septal defect (primum or secundum) altered the PQ interval of the wild-type or *Tbx5*$^{del/+}$ newborn mice **(**ASD primum 50.7±5.6 ms vs. ASD secundum 52.5±5.3 ms; P-value not significant).

Comparison of PQ intervals in neonatal and adult wild-type mice demonstrates that the time required for electrical propagation from sinoatrial node to ventricular myocardium (Fig. 3A) normally decreases with maturation, even though the signal must travel further in the larger adult heart. In wild-type mice, the PQ interval becomes significantly shorter between

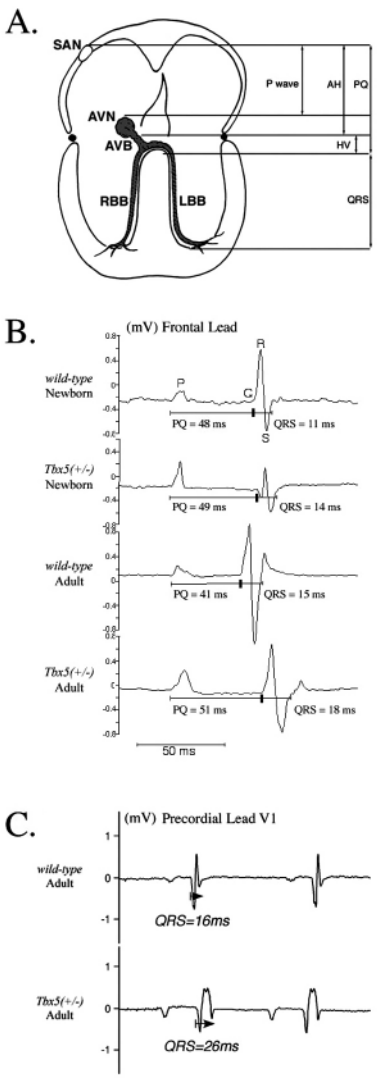

Fig. 3. PQ maturation defect and QRS prolongation in *Tbx5*$^{del/+}$ mice. (A) Schematic representation of electrical impulse propagation through the mammalian heart correlated with surface ECG and in-vivo electrophysiology intervals. PQ intervals include impulse propagation throughout the atria and atrioventricular node (proximal AH interval) and the atrioventricular bundle and proximal bundle branches (distal HV interval). P-wave duration represents atrial depolarization. QRS intervals represent ventricular activation, and include bundle branch and Purkinje conduction. Bundle-branch block causes QRS prolongation with characteristic ECG wave front morphology. SAN, sinoatrial node; AVN, atrioventricular node; AVB, atrioventricular bundle; RBB, right bundle branch; LBB, left bundle branch. (B) Representative ECGs from wild-type and *Tbx5*$^{del/+}$ newborns and adult mice. Note comparable PQ intervals (atrial plus atrioventricular canal conduction time) in neonatal wild-type and *Tbx5*$^{del/+}$ mice. Adult wild-type mice had significantly shorter PQ intervals than those of *Tbx5*$^{del/+}$ mice. QRS intervals of newborn and adult *Tbx5*$^{del/+}$ mice were longer than in wild-type mice (Table 1). (C) Representative ECG recordings from right precordial leads (V1) in wild-type and *Tbx5*$^{del/+}$ adult mouse. Wild-type mice had normal QRS complexes. *Tbx5*$^{del/+}$ mice had QRS prolongation with a RSR′ wave front pattern indicative of RBB. RBB occurred in 9 of 11 of adult *Tbx5*$^{del/+}$ mice versus 3 of 27 adult wild-type mice (P<0.001).

the newborn and adult periods (48.0±7.6 ms vs. 41.9±1.0 ms; P<0.001) (Fig. 3B, Table 1). However, in *Tbx5*$^{del/+}$ mice, the PQ interval does not change significantly between the newborn and adult periods (50.7±5.8 ms vs. 49.1±4.6 ms; P<0.46) (Fig. 3B, Table 1), suggesting that a failure of normal maturation accounts for the prolonged PR interval in adult *Tbx5*$^{del/+}$ mice.

In-vivo electrophysiology studies were performed in adult animals to localize the functional deficit in *Tbx5*$^{del/+}$ mice to the atrium, atrioventricular node, or the atrioventricular bundle and proximal bundle branches. The AH interval (representing conduction propagation through the atrium and the atrioventricular node) and the HV interval (representing conduction propagation through the atrioventricular bundle and proximal bundle branches) were measured separately (Fig. 3A). The HV interval of adult *Tbx5*$^{del/+}$ mice and wild-type mice were not significantly different (10.3±2.0 ms vs. 11.5±1.5 ms; P<0.69; n=6). However, the AH interval of adult *Tbx5*$^{del/+}$ mice was significantly longer than the AH interval of adult wild-type mice (42.3±6.0 ms vs. 37.0±1.5 ms; P<0.001; n=6), demonstrating a functional deficit of atrial or atrioventricular node conduction in adult *Tbx5*$^{del/+}$ mice. To distinguish between these, propagation of the electrical signal in the atria (atrial depolarization or P-wave) was directly measured by analyzing P-wave duration. P-wave duration was not significantly different between adult *Tbx5*$^{del/+}$ mice and wild-type mice (15.9±2.5 ms vs. 15.0±1.1 ms; P<0.36; n=12). Taken together, the normal P-wave duration and AH interval prolongation suggests that the PQ prolongation in *Tbx5*$^{del/+}$ mice is the result of a defect of the atrioventricular node or its connection with the atria or atrioventricular bundle.

Tbx5 haploinsufficiency causes atrioventricular bundle and bundle branch conduction system patterning defects

We used β-galactosidase activity in *minK*$^{lacZ/+}$ mice to characterize the morphology of the postnatal ventricular conduction system, including the atrioventricular bundle and bundle branches. The left bundle branch, lying on the left side of the interventricular septum, was identified in all newborn *minK*$^{lacZ/+}$ mouse hearts (n=25), as a broad sheet of cells with β-galactosidase activity (Fig. 4B, arrowhead). This pattern was consistent with classic histological descriptions of the left bundle branch in young mouse hearts (Fig. 4B) (Lev and Thaemert, 1973). In all adult *minK*$^{lacZ/+}$ mouse hearts (n=18), β-galactosidase activity was more discretely concentrated into a bundle branch fascicle. In all adult *minK*$^{lacZ/+}$ mouse hearts (n=18), β-galactosidase activity also demarcated a well-defined atrioventricular bundle, located on the crest of the interventricular septum (Fig. 4C, red arrowhead).

The effect of *Tbx5* haploinsufficiency on atrioventricular bundle and left ventricular bundle branch morphology was evaluated in *Tbx5*$^{del/+}$/*minK*$^{lacZ/+}$ mice (Fig. 4). In all newborn *Tbx5*$^{del/+}$/*minK*$^{lacZ/+}$ hearts (n=22), β-galactosidase activity in the left ventricle was indistinguishable from that in newborn *minK*$^{lacZ/+}$ hearts (Fig. 4D). By contrast, in adult *Tbx5*$^{del/+}$/*minK*$^{lacZ/+}$ hearts, β-galactosidase activity (Fig. 4E) was present in a broader sheet of cells, exhibiting a pattern reminiscent of the immature left bundle branch conduction system. Absence of a consolidated, discrete band of cells in the left ventricular bundle branch was found in all adult *Tbx5*$^{del/+}$/*minK*$^{lacZ/+}$ hearts examined (n=15). Furthermore, the

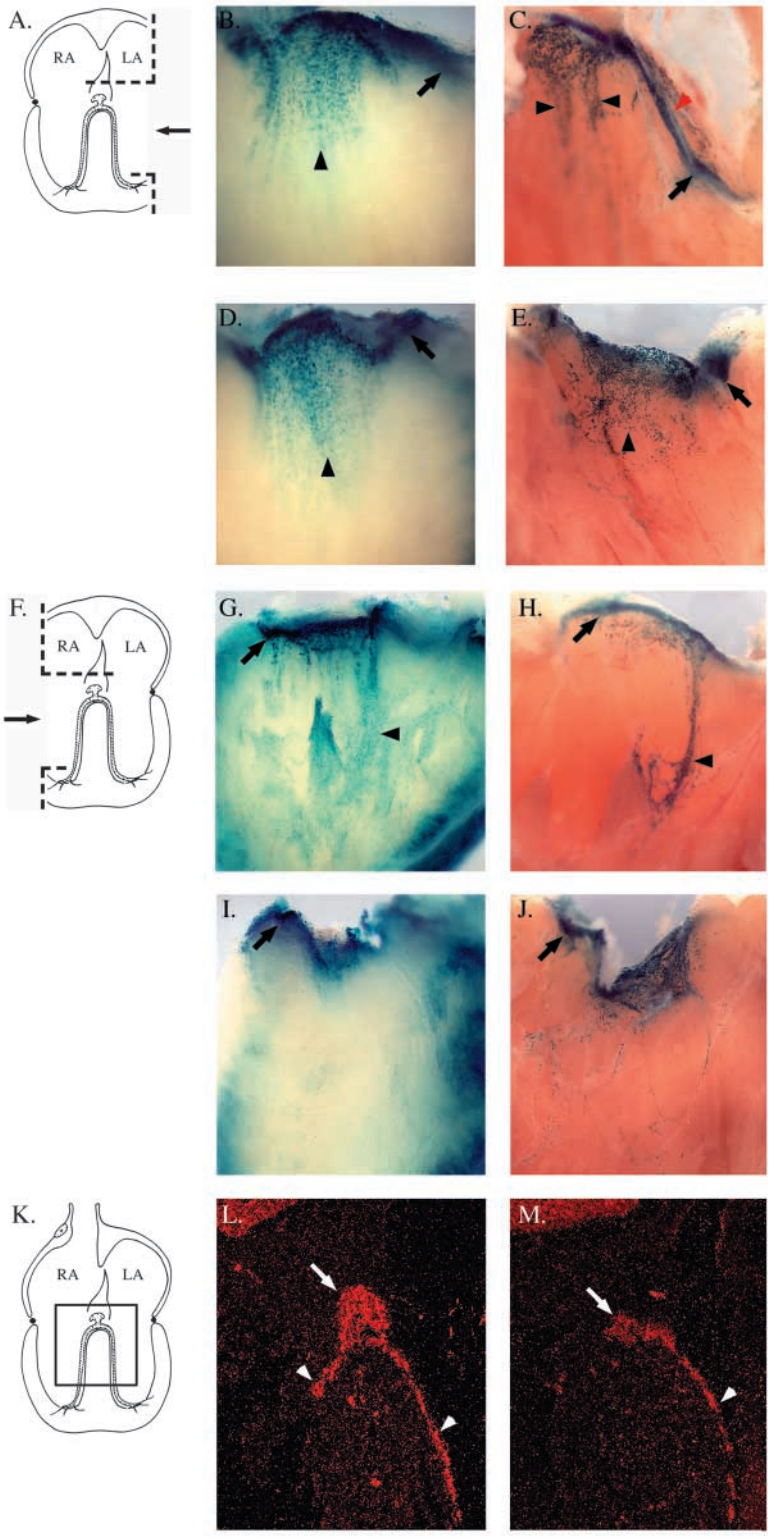

Fig. 4. Bundle-branch patterning defects in *Tbx5*$^{del/+}$ mice. (A) Schematic representation of dissection of left-bundle-branch conduction system showing the plane of dissection (dashed line) and specimen orientation (arrow). The left ventricular free wall and mitral valve were removed to view the interventricular septum from the left. β-Galactosidase expression marked the left-bundle-branch conduction system in *minK*$^{lacZ/+}$ (B,C) and *Tbx5*$^{del/+}$/*minK*$^{lacZ/+}$ (D,E) mouse hearts. The atrioventricular node (black arrow), atrioventricular bundle (red arrowhead) and left bundle branch (black arrowhead) were visible on the surface of the muscular interventricular septum. The broad left bundle branch in newborn *minK*$^{lacZ/+}$ mice (B) matured into a narrow fascicle with a well-defined atrioventricular bundle (red arrowhead) in adult *minK*$^{lacZ/+}$ mice (C). Comparable maturation did not occur in *Tbx5*$^{del/+}$/*minK*$^{lacZ/+}$ mice (D,E) and adult *Tbx5*$^{del/+}$/*minK*$^{lacZ/+}$ mice (E) retained the broad band of specialized conduction cells, without a discrete atrioventricular bundle. (F) Schematic representation of dissection of right-bundle-branch conduction system showing the plane of dissection (dashed line) and specimen orientation (arrow). The right ventricular free wall and tricuspid valve were removed and the interventricular septum viewed from the right. β-Galactosidase expression marked the right bundle branch in *minK*$^{lacZ/+}$ (G,H) and *Tbx5*$^{del/+}$ *minK*$^{lacZ/+}$ (I,J) mouse hearts. The atrioventricular node (black arrow) and right bundle branch (black arrowhead) were visible on the surface of the muscular interventricular septum. In newborn *minK*$^{lacZ/+}$ mouse hearts (G), the right bundle branch was visible as a poorly defined band of cells loosely associated with the septal band and anterior papillary muscle of the right ventricle. In adult *minK*$^{lacZ/+}$ mouse hearts (H), the right bundle branch was well defined by a thin band of cells running along the inferior aspect of the septal band and onto the anterior papillary muscle of the right ventricle. In 9/20 newborn (I) and 7/15 adult (J) *Tbx5*$^{del/+}$/*minK*$^{lacZ/+}$ mouse hearts, the right bundle branch was absent from the right ventricular septal surface, with conduction cells present only along the crest of the interventricular septum demarcating the atrioventricular bundle. (K) Schematic representation of dissection of the interventricular septum for images in (L,M). In-situ hybridization with a connexin 40 probe in wild-type (L) and *Tbx5*$^{del/+}$ (M) mouse hearts. Connexin 40 expression was observed in the atrioventricular bundle (arrow), and left and right bundle branches (arrowheads) in the wild-type mouse heart (L) and in the atrioventricular bundle (arrow) and left bundle branch but not the right bundle branch in the *Tbx5*$^{del/+}$ mouse heart (M). In 3/5 newborn *Tbx5*$^{del/+}$/*minK*$^{lacZ/+}$ mouse hearts, the right bundle branch could not be identified.

atrioventricular bundle appeared foreshortened in all adult *Tbx5*$^{del/+}$/*minK*$^{lacZ/+}$ hearts examined (n=15).

The right bundle branch, present on the surface of the right side of the interventricular septum, had a different structure than that of the left bundle branch (Fig. 4F-H). In newborn *minK*$^{lacZ/+}$ mouse hearts (n=25), β-galactosidase activity identified a loose bundle of cells adjacent to the septal band and anterior papillary muscle of the right ventricle, consistent with classic histological descriptions (Lev and Thaemert, 1973) of the right bundle branch (Fig. 4G). The right bundle branch in adult *minK*$^{lacZ/+}$ mouse hearts (Fig. 4H) was more well-defined than that in newborn mice, displaying a highly stereotyped pattern in all 18 hearts examined that was remarkably analogous to that of the adult human right bundle branch.

Severe patterning defects of the right bundle branch were observed in newborn and adult *Tbx5*$^{del/+}$/*minK*$^{lacZ/+}$ mice. In all newborn *Tbx5*$^{del/+}$/*minK*$^{lacZ/+}$ mouse hearts studied (*n*=22), there was a paucity of cells with β-galactosidase activity in the right ventricle. The most severe cases (10/22 hearts) had complete absence of a discrete right bundle branch on the right ventricular septal surface (Fig. 4I). In less severe cases (12/22 hearts), the right bundle branch was foreshortened and failed to associate with the anterior papillary muscle (data not shown).

As in neonates, adult *Tbx5*$^{del/+}$/*minK*$^{lacZ/+}$ mouse hearts exhibited markedly abnormal right bundle branches. In 15 hearts examined, there was a marked paucity of β-galactosidase-expressing cells on the right ventricular septal surface. In 8 of 15 hearts, the right bundle branch was entirely missing, and only a few dispersed cells with β-galactosidase activity could be identified on the right ventricular septal surface (Fig. 4J). In the remaining mutant hearts (*n*=7), a foreshortened right bundle branch was present (not shown).

To verify the severe bundle-branch-patterning defects observed in *Tbx5*$^{del/+}$/*minK*$^{lacZ/+}$ mouse hearts, conduction system morphology in *Tbx5*$^{del/+}$ newborn mouse hearts was also evaluated by in-situ hybridization of connexin 40 expression on sagital sections. In wild-type newborn mouse hearts (*n*=6), connexin 40 expression uniformly marked the atrioventricular bundle and left and right bundle branches (Fig. 4L). In *Tbx5*$^{del/+}$ newborn mouse hearts (*n*=6), connexin 40 was also observed in the atrioventricular bundle and left bundle branch (Fig. 4M). However, no right bundle branch could be identified in 3/5 *Tbx5*$^{del/+}$ newborn hearts (Fig. 4M). In these cases, a right bundle branch was absent even from the region adjacent to the membranous septum, where the right bundle branch normally exits the atrioventricular bundle to enter the right ventricle (Fig. 4M).

To assess the functional consequences of the profound bundle branch morphologic abnormalities in *Tbx5*$^{del/+}$ mice, ventricular conduction was evaluated using surface ECG analysis. Previous studies using single lead Holter monitoring revealed no ventricular conduction differences between wild-type and *Tbx5*$^{del/+}$ mice (Bruneau et al., 2001). Using 6-lead ECGs, we found that the QRS interval, produced by depolarization and activation of the ventricular myocardium (Surawicz and Knilans, 2001a), was significantly longer in *Tbx5*$^{del/+}$ mice than that in wild-type mice. QRS prolongation occurred both in neonates (12.7±2.6 ms vs. 9.8±1.5 ms; *P*<0.001) and in adults (16.5±1.0 ms vs. 13.7±1.3 ms; *P*<0.005) (Fig. 3B; Table 1B). Neither the *minK*$^{lacZ/+}$ allele nor the type of septal defect (primum or secundum) had a significant effect on the QRS interval of the wild-type or *Tbx5*$^{del/+}$ neonatal or adult mice **(**ASD primum 16.8±0.9 ms versus ASD secundum 16.3±3.2 ms; *P*-value not significant).

Delay or loss of conduction through one of the bundle branches, termed 'bundle-branch block', results in lengthening of the QRS interval due to delayed and asynchronous activation of the ventricular myocardium contralateral to the affected bundle branch (Surawicz and Knilans, 2001b) (Fig. 3A). To ascertain whether QRS prolongation in *Tbx5*$^{del/+}$ mice was due to a bundle-branch block, surface 6-limb ECGs with a right precordial lead were recorded. The QRS complex recorded from the right precordial lead has a distinct morphology in the case of either right or left bundle branch, allowing their unique identification (Surawicz and Knilans, 2001b). An RSr′ morphology indicative of right-bundle-branch block was observed in 9/11 *Tbx5*$^{del/+}$ mice versus 3/27 adult wild-type mice (*P*<0.001) (Fig. 3C). RSr′ is the standard notation for a notched QRS upstroke (an initial upward deflection (R) followed by a downward deflection (S) followed by another upward deflection (r′)). RSr′ morphology on ECG combined with prolongation of QRS duration is indicative of right-bundle-branch block. The type of atrial septal defect in the heart (secundum or primum) had no significant effect on the likelihood of right-bundle-branch block in *Tbx5*$^{del/+}$ adult mice **(**ASD primum 4/4 vs. ASD secundum 5/7; *P*-value not significant).

To determine whether the developmental failure of a morphologic right bundle branch correlated with the ECG finding of right-bundle-branch block, structure and function were assessed in 10 *Tbx5*$^{del/+}$ mice. All (*n*=4) mice with morphologic absence of the right bundle branch demonstrated right-bundle-branch block by precordial ECG analysis. By contrast, only 2/6 mice with a morphologically visible right bundle branch demonstrated a right-bundle-branch block on ECG.

Normal conduction system patterning in mice lacking *Cx40*, a *Tbx5*-target gene

Previous studies demonstrated that *Cx40*, which encodes a gap junction protein required for normal conduction system function, is a gene target of *Tbx5*. Adult *Tbx5*$^{del/+}$ mice express only 10% of normal levels of *Cx40* transcripts, and Tbx5 directly binds and activates the *Cx40* promoter in primary cultures of cardiomyocytes (Bruneau et al., 2001). *Cx40* null mice (*Cx40*$^{-/-}$) have prolonged PQ intervals, prolonged QRS intervals, and right-bundle-branch block (Kirchhoff et al., 1998; Simon et al., 1998; Bevilacqua et al., 2000; Saffitz and Schuessler, 2000; Tamaddon et al., 2000; van Rijen et al., 2001).

To test whether *Cx40* insufficiency accounted for the morphologic and electrophysiologic defects in the conduction system of *Tbx5*$^{del/+}$ mice, we studied *Cx40*$^{-/-}$ mice (Simon et al., 1998). The morphology of the conduction system was analyzed in compound *Cx40*$^{-/-}$/*minK*$^{lacZ/+}$ mice by evaluating β-galactosidase activity in adult hearts (Fig. 5). Precordial ECG analyses confirmed previously described electrophysiologic abnormalities: 19/19 *Cx40*$^{-/-}$ mice had a prolonged PR interval and 15/19 had a right-bundle-branch block (data not shown). Morphologic analyses were performed in mice with the most severe ECG abnormalities, those with prolonged PR interval and right-bundle-branch block. The atrioventricular node, atrioventricular bundle, left bundle branch and right bundle branch identified by β-galactosidase activity were well-formed and normally patterned in all *Cx40*$^{-/-}$/*minK*$^{lacZ/+}$ mice (*n*=10) (Fig. 5A-F). Both the amount and the distribution of β-galactosidase activity were indistinguishable from that observed in littermate *minK*$^{lacZ/+}$ mice (Fig. 5).

Discussion

Our findings demonstrate a critical role for *Tbx5* in development of the specialized electrophysiologic system of the heart. *Tbx5* is expressed in the central conduction system including the atrioventricular node, atrioventricular bundle and ventricular bundle branches. In the atrioventricular canal, *Tbx5* has specific roles in postnatal morphologic and functional maturation of the atrioventricular node and atrioventricular

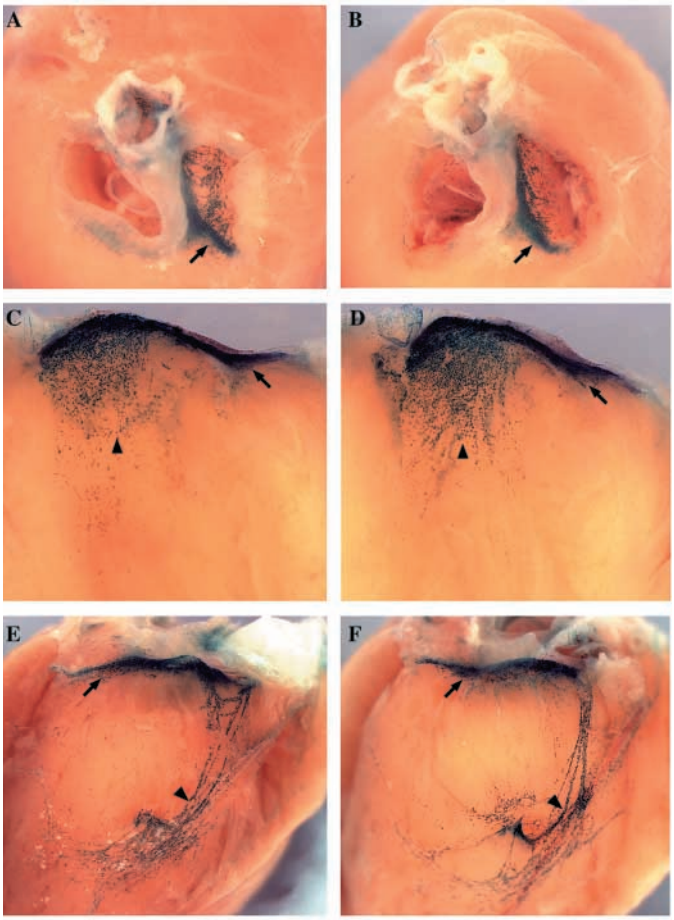

Fig. 5. Normal conduction system morphology in *Cx40*$^{-/-}$ mice. β-Galactosidase expression in *minK*$^{lacZ/+}$ (A,C,E) and *Cx40*$^{-/-}$/*minK*$^{lacZ/+}$ (B,D,F) mouse hearts. In the atrioventricular canal, a well-defined atrioventricular node (arrow) and atrioventricular bundle were observed in both *minK*$^{lacZ/+}$ (A) and *Cx40*$^{-/-}$/*minK*$^{lacZ/+}$ (B) mouse hearts. The atria were removed and the atrioventricular canal was viewed from the superior/posterior, with the tricuspid annulus on the right and the mitral annulus on the left. A well-formed left bundle branch was found in both *minK*$^{lacZ/+}$ (C) and *Cx40*$^{-/-}$/*minK*$^{lacZ/+}$ (D) mouse hearts. The left ventricular free wall and mitral valve were removed and the left interventricular septum viewed from the left. A well-formed right bundle branch was present in *minK*$^{lacZ/+}$ (E) and *Cx40*$^{-/-}$/*minK*$^{lacZ/+}$ (F) mouse hearts. The right ventricular free wall and tricuspid valve were removed and the right interventricular septum viewed from the right. Comparable β-galactosidase expression and morphology were demonstrated in 12/12 *minK*$^{lacZ/+}$ and 10/10 *Cx40*$^{-/-}$/*minK*$^{lacZ/+}$ mice.

bundle. In the ventricular conduction system, *Tbx5* is required for morphologic maturation of the atrioventricular bundle and left bundle branch and is essential for the patterning and function of the right bundle branch.

Tbx5 expression and specification of central conduction system cells

Early in embryogenesis, *Tbx5* is expressed throughout the cardiac crescent, but becomes restricted during formation of the linear heart tube. High levels persist in the atria, but *Tbx5* levels in the primordial ventricles decrease throughout gestation, and prior to birth *Tbx5* expression is largely restricted to the endocardial surface of the left ventricle. By contrast, Tbx5 levels in the atrioventricular bundle and bundle branches (Fig. 1) are maintained at birth, and levels in these conduction system structures are higher than in the surrounding ventricular myocardium (Fig. 1). *Tbx5* is also known to activate the promoters of genes encoding the gap junction proteins Cx40 and ANF (Bruneau et al., 2001), two molecules that distinguish adult electrophysiologic cells from working myocardial cells of the ventricle (Houweling et al., 2002; Coppen et al., 2003). The temporal and spatial pattern of *Tbx5* expression and transcriptional activity is consistent with a role for this transcription factor in specification of the conduction system cells.

Tbx5 is required for maturation of the atrioventricular canal conduction system

Development of the mature conduction system requires both specification of cells with electrophysiologic functions and morphologic patterning of the central and peripheral electrophysiologic components. Organization of specialized electrophysiologic cells into distinct components of the mature conduction system appears to occur in distinct temporal steps. Some cells in the central conduction system appear to be specified early in development, since node-like pacemaker activity is evident by the linear-heart-tube stage (Kamino et al., 1981). Differentiation of the fast-conducting atrioventricular bundle and bundle branches occurs later in embryogenesis (Delorme et al., 1995; Sedmera et al., 2003). Analysis of *minK*$^{lacZ/+}$ mice (Fig. 2A,B) extends the temporal sequence for central conduction system development into the postnatal period. At birth, rings of conduction tissue persist around both the tricuspid annulus and mitral annulus. Consolidation of electrophysiologic cells into a discrete atrioventricular node, atrioventricular bundle and bundle branches, the pattern of a mature conduction system, is a postnatal process that in the mouse is completed by week 14.

Although the rings of specialized electrophysiologic tissue are similar in newborn *minK*$^{lacZ/+}$ mice and *Tbx5*$^{del/+}$ mice, postnatal maturation of the atrioventricular canal conduction system fails to occur in *Tbx5*$^{del/+}$ mice. Adult *Tbx5*$^{del/+}$ mice maintain a neonatal pattern of specialized atrioventricular rings around both the tricuspid annulus and mitral annulus. The failure of morphologic atrioventricular canal maturation correlates with functional immaturity of the atrioventricular conduction system: absence of the normal age-dependent decrease of the PQ interval results in age-dependent atrioventricular block in *Tbx5*$^{del/+}$ mice (Fig. 3).

In-vivo electrophysiology localized the anatomic source of the PQ prolongation in adult *Tbx5*$^{del/+}$ mice. The PQ interval encompasses electrical conduction within the atrial musculature, atrioventricular node, atrioventricular bundle and proximal bundle branches (Fig. 3A). The normal HV interval in *Tbx5*$^{del/+}$ mice suggests that the atrioventricular bundle has normal function, despite appearing physically foreshortened (Table 1, Fig. 4). The prolonged AH interval in *Tbx5*$^{del/+}$ mice placed the functional defect in the atrial myocardium or atrioventricular node. Furthermore, a normal P-wave duration, indicative of atrial depolarization, ruled out a functional deficit within the atrial myocardium (Table 1). From these findings, we infer that the prolonged PQ interval in *Tbx5*$^{del/+}$ mice is the result of a maturation failure of the atrioventricular node or its connection with the atria or atrioventricular bundle. This finding

could also reflect a deficit in one of the distinct subpopulations of cells within the atrioventricular node (Coppen et al., 2003).

Progressive atrioventricular block is found in human Holt–Oram syndrome. Conduction system disease is unusual at birth, but first or second-degree atrioventricular block occurs commonly in adult patients. The progressive onset of atrioventricular canal conduction dysfunction in humans and mice with *Tbx5* haploinsufficiency suggests that the same postnatal *Tbx5*-dependent processes are required for the maturation of the atrioventricular canal conduction system in mice and humans.

Tbx5 and the ventricular conduction system

Tbx5 is also required for normal patterning and function of the proximal ventricular conduction system, the atrioventricular bundle and the left and right bundle branches. In adult *Tbx5*$^{del/+}$ mouse hearts, each of these components demonstrates a morphologic patterning defect (Fig. 4). The fast-conducting ventricular conduction system also demonstrates a functional deficit of the right bundle branch but not the left bundle branch (Table 1). We conclude that the patterning of the right bundle branch is sufficiently disrupted to cause malfunction, whereas patterning of the left bundle branch is not. Furthermore, deficits in the right bundle branch are visible at birth (Fig. 4). These findings define a role for Tbx5 in the development of the right bundle branch and suggest a substantial role in the differentiation of the components of the fast-conducting ventricular conduction system, including the atrioventricular bundle. Distinct differences in these components of the central conduction system in newborn *Tbx5*$^{del/+}$ mouse hearts suggest that development of the atrioventricular node, atrioventricular bundle and bundle branches have distinct molecular requirements. These data are consistent with a model in which regional components of the conduction system are specified independently and are then assembled into a continuous network.

Complete absence or a diminutive right bundle branch was found in all *Tbx5*$^{del/+}$ mice, indicating that normal levels of the transcription factor are essential for genesis of this structure. As in the atrioventricular canal, the morphologic deficits of the bundle-branch conduction system were mirrored by functional defects. In particular, there was a close correlation between the severity of the right-bundle-branch morphology defects and functional right-bundle-branch block in *Tbx5*$^{del/+}$*/minK*$^{lacZ/+}$ mice. All mice with morphologic absence of the right bundle branch had right-bundle-branch block by precordial ECG, whereas few mice with a visible right bundle branch demonstrated right-bundle-branch block. These data suggest that a functional electrophysiological deficit in *Tbx5*$^{del/+}$ mice occurred as a consequence of an underlying primary, maldeveloped morphology in the conduction system.

Tbx5 haploinsufficiency directly disrupts the central conduction system

Several lines of evidence suggest that malformation of the central cardiac conduction system in *Tbx5*$^{del/+}$ mice occurs independent of cardiac structural defects. First, despite an intact ventricular septum, all *Tbx5*$^{del/+}$ mice had malformations in the ventricular conduction system, usually affecting both the right and left bundle branches. Second, there was no relationship between the specific type of ASD in *Tbx5*$^{del/+}$ mice and conduction system abnormalities. The presence of a secundum or primum ASD did not correlate with the severity of morphologic defects in the central conduction system, and no statistically significant differential effect was observed on the PQ interval, QRS interval or likelihood of right-bundle-branch block (Table 1). We conclude that *Tbx5* has a direct role in conduction system development independent of its role in structural heart development. Furthermore, the finding that *Tbx5* is expressed at high levels in conduction system cells suggests that its conduction system requirement may be cell-autonomous.

Cx40, a transcriptional target of *Tbx5* that encodes a gap junction protein required for normal electrophysiologic function of the heart, was considered a potential cause for the patterning defects evident in the central conduction system of *Tbx5*$^{del/+}$ mice. Like *Tbx5*$^{del/+}$ mice, *Cx40*$^{-/-}$ mice demonstrate prolonged PQ intervals, prolonged QRS intervals, and in some cases right-bundle-branch block (data not shown) (Kirchhoff et al., 1998; Simon et al., 1998; Tamaddon et al., 2000). The degree to which the decrement in *Cx40* transcription in *Tbx5*$^{del/+}$ mice accounts for the functional conduction system abnormalities in *Tbx5*$^{del/+}$ mice remains unclear. Our recent findings demonstrate the critical importance of even limited *Cx40* expression in *Tbx5*$^{del/+}$ mice: whereas *Tbx5*$^{del/+}$ mice usually live to adulthood, *Tbx5*$^{del/+}$*/Cx40*$^{-/-}$ mice die in utero (A.P., unpublished).

Cx40 deficiency does not, however, explain the morphologic abnormalities of the central conduction system found in *Tbx5*$^{del/+}$ mice. Normal morphology of the atrioventricular node, atrioventricular bundle and bundle branches was present in all adult *Cx40*$^{-/-}$ mice, indicating that this gap junction protein is not required for the morphologic maturation or patterning of the central conduction system. These findings implicate yet unidentified genes downstream of *Tbx5* in the patterning of the conduction system.

Our results delineate several distinct roles for *Tbx5* in conduction system development. Early in cardiac development, the temporal and spatial expression of *Tbx5* is compatible with a role in specification of cells in the conduction system. *Tbx5*-dependent expression of *Cx40*, and presumably other molecules that are required for the critical electrophysiologic properties of these cells, supports this hypothesis. *Tbx5* directs the expression of genes (e.g. *Cx40*) in the mature conduction system, after the primitive AV node, left bundle branch and right bundle branch have assumed their adult structures, which may account for why some Holt-Oram patients and *Tbx5*$^{del/+}$ mice evolve conduction system disease with age. In addition to regulating gene transcription in the conduction system, *Tbx5*, but not *Cx40*, is critical for conduction system pattern formation. Normal morphology of the atrioventricular canal components and ventricular components of central conduction system are dependent on physiologic levels of this factor. *Tbx5* is the first gene to be implicated in the pattern formation and the developmental maturation of the centralized cardiac conduction system. A link between a patterning abnormality of the developing conduction system and a functional abnormality of the mature conduction system is demonstrated.

We wish to thank Dr David Paul for the use of connexin 40 knockout mice and Michael Peterson for excellent technical assistance. This work was supported by funding from the Howard Hughes Medical Institute. I.P.G.M. was supported by a Howard Hughes Medical Institute Physician Postdoctoral Fellowship.

References

Bamshad, M., Lin, R. C., Law, D. J., Watkins, W. C., Krakowiak, P. A., Moore, M. E., Franceschini, P., Lala, R., Holmes, L. B., Gebuhr, T. C. et al. (1997). Mutations in human TBX3 alter limb, apocrine and genital development in ulnar-mammary syndrome. *Nat. Genet.* **16**, 311-315.

Basson, C. T., Bachinsky, D. R., Lin, R. C., Levi, T., Elkins, J. A., Soults, J., Grayzel, D., Kroumpouzou, E., Traill, T. A., Leblanc-Straceski, J. et al. (1997). Mutations in human TBX5 cause limb and cardiac malformation in Holt-Oram syndrome. *Nat. Genet.* **15**, 30-35.

Basson, C. T., Cowley, G. S., Solomon, S. D., Weissman, B., Poznanski, A. K., Traill, T. A., Seidman, J. G. and Seidman, C. E. (1994). The clinical and genetic spectrum of the Holt-Oram syndrome (heart-hand syndrome). *New Engl. J. Med.* **330**, 885-891.

Basson, C. T., Huang, T., Lin, R. C., Bachinsky, D. R., Weremowicz, S., Vaglio, A., Bruzzone, R., Quadrelli, R., Lerone, M., Romeo, G. et al. (1999). Different TBX5 interactions in heart and limb defined by Holt-Oram syndrome mutations. *Proc. Natl. Acad. Sci. USA* **96**, 2919-2924.

Berul, C. I., Aronovitz, M. J., Wang, P. J. and Mendelsohn, M. E. (1996). In vivo cardiac electrophysiology studies in the mouse. *Circulation* **94**, 2641-2648.

Berul, C. I., McConnell, B. K., Wakimoto, H., Moskowitz, I. P., Maguire, C. T., Semsarian, C., Vargas, M. M., Gehrmann, J., Seidman, C. E. and Seidman, J. G. (2001). Ventricular arrhythmia vulnerability in cardiomyopathic mice with homozygous mutant myosin binding protein C gene. *Circulation* **104**, 2734-2739.

Bevilacqua, L. M., Simon, A. M., Maguire, C. T., Gehrmann, J., Wakimoto, H., Paul, D. L. and Berul, C. I. (2000). A targeted disruption in Connexin40 leads to distinct atrioventricular conduction defects. *J. Intervent. Cardiac Electrophysiol.* **4**, 459-467.

Bruneau, B. G., Logan, M., Davis, N., Levi, T., Tabin, C. J., Seidman, J. G. and Seidman, C. E. (1999). Chamber-specific cardiac expression of Tbx5 and heart defects in Holt-Oram syndrome. *Dev. Biol.* **211**, 100-108.

Bruneau, B. G., Nemer, G., Schmitt, J. P., Charron, F., Robitaille, L., Caron, S., Conner, D. A., Gessler, M., Nemer M., Seidman, C. E. et al. (2001). A murine model of Holt-Oram syndrome defines roles of the T-box transcription factor Tbx5 in cardiogenesis and disease. *Cell* **106**, 709-721.

Cheng, C. F., Kuo, H. C. and Chien, K. R. (2003). Genetic modifiers of cardiac arrhythmias. *Trends Mol. Med.* **9**, 59-66.

Coppen, S. R., Severs, N. J. and Gourdie, R. G. (1999). Connexin45 (alpha 6) expression delineates an extended conduction system in the embryonic and mature rodent heart. *Dev. Genet.* **24**, 82-90.

Coppen, S. R., Kaba, R. A., Halliday, D., Dupont, E., Skepper, J. N., Elneil, S. and Severs, N. J. (2003). Comparison of connexin expression patterns in the developing mouse heart and human foetal heart. *Mol. Cell. Biochem.* **242**, 121-127.

Davis, D. L., Edwards, A. V., Juraszek, A. L., Phelps, A., Wessels, A. and Burch, J. B. (2001). A GATA-6 gene heart-region-specific enhancer provides a novel means to mark and probe a discrete component of the mouse cardiac conduction system. *Mech. Dev.* **108**, 105-119.

Delorme, B., Dahl, E., Jarry-Guichard, T., Marics, I., Briand, J. P., Willecke, K., Gros, D. and Theveniau-Ruissy, M. (1995). Developmental regulation of connexin 40 gene expression in mouse heart correlates with the differentiation of the conduction system. *Dev. Dyn.* **204**, 358-371.

Gehrmann, J. and Berul, C. I. (2000). Cardiac electrophysiology in genetically engineered mice. *J. Cardiovasc. Electrophysiol.* **11**, 354-368.

Gourdie, R. G., Harris, B. S., Bond, J., Justus, C., Hewett, K. W., O'Brien, T. X., Thompson, R. P. and Sedmera, D. (2003). Development of the cardiac pacemaking and conduction system. *Birth Defects Res. Part C Embryo Today* **69**, 46-57.

Hatcher, C. J., Goldstein, M. M., Mah, C. S., Delia, C. S. and Basson, C. T. (2000). Identification and localization of TBX5 transcription factor during human cardiac morphogenesis. *Dev. Dyn.* **219**, 90-95.

Herrmann, B. G., Labeit, S., Poustka, A., King, T. R. and Lehrach, H. (1990). Cloning of the T gene required in mesoderm formation in the mouse. *Nature* **343**, 617-622.

Houweling, A. C., Somi, S., Van Den Hoff, M. J., Moorman, A. F. and Christoffels, V. M. (2002). Developmental pattern of ANF gene expression reveals a strict localization of cardiac chamber formation in chicken. *Anat. Rec.* **266**, 93-102.

Kamino, K., Hirota, A. and Fujii, S. (1981). Localization of pacemaking activity in early embryonic heart monitored using voltage-sensitive dye. *Natur*e **290**, 595-597.

Kirchhoff, S., Nelles, E., Hagendorff, A., Kruger, O., Traub, O. and Willecke, K. (1998). Reduced cardiac conduction velocity and predisposition to arrhythmias in connexin40-deficient mice. *Curr. Biol.* **8**, 299–302.

Kondo, R. P., Anderson, R. H., Kupershmidt, S., Roden, D. M. and Evans, S. M. (2003). Development of the cardiac conduction system as delineated by minK-lacZ. *J. Cardiovasc. Electrophysiol.* **14**, 383-391.

Kupershmidt, S., Yang, T., Anderson, M. E., Wessels, A., Niswender, K. D., Magnuson, M. A. and Roden, D. M. (1999). Replacement by homologous recombination of the minK gene with lacZ reveals restriction of minK expression to the mouse cardiac conduction system. *Circ. Res.* **84**, 146-152.

Lev, M. and Thaemert, J. C. (1973). The conduction system of the mouse heart. *Acta Anat. (Basel)* **85**, 342-352.

Li, Q. Y., Newbury-Ecob, R. A., Terrett, J. A., Wilson, D. I., Curtis, A. R., Yi, C. H., Gebuhr, T., Bullen, P. J., Robson, S. C., Strachan, T. et al. (1997). Holt-Oram syndrome is caused by mutations in TBX5, a member of the Brachyury (T) gene family. *Nat. Genet.* **15**, 21-29.

Maguire, C. T., Bevilacqua, L. M., Wakimoto, H., Gehrmann, J. and Berul, C. I. (2000). Maturational atrioventricular nodal physiology in the mouse. *J. Cardiovasc. Electrophysiol.* **11**, 557-564.

Marriott, H. J. L. and Conover, M. B. (1998). *Advanced Concepts in Arrhythmias*. 3rd edn, p.33. St Louis, MO: Mosby.

Merscher, S., Funke, B., Epstein, J. A., Heyer, J., Puech, A., Lu, M. M., Xavier, R. J., Demay, M. B., Russell, R. G. and Factor, S. (2001). TBX1 is responsible for cardiovascular defects in velo-cardio-facial/DiGeorge syndrome. *Cell* **104**, 619-629.

Moorman, A. F., de Jong, F., Denyn, M. M. and Lamers, W. H. (1998). Development of the cardiac conduction system. *Circ. Res.* **82**, 629-644.

Muller, C. W. and Herrmann, W. H. (1997). Crystallographic structure of the T domain-DNA complex of the Brachyury transcription factor. *Nature* **389**, 695–697.

Newbury-Ecob, R. A., Leanage, R., Raeburn, J. A. and Young, I. D. (1996). Holt-Oram syndrome: a clinical genetic study. *J. Med. Genet.* **33**, 300-307.

Nguyen-Tran, V. T., Kubalak, S. W., Minamisawa, S., Fiset, C., Wollert, K. C., Brown, A. B., Ruiz-Lozano, P., Barrere-Lemaire, S., Kondo, R., Norman, L. W. et al. (2000). A novel genetic pathway for sudden cardiac death via defects in the transition between ventricular and conduction system cell lineages. *Cell* **102**, 671-682.

Papaioannou, V. E. and Silver, L. M. (1998). The T-box gene family. *BioEssays* **20**, 9-19.

Saffitz, J. E. and Schuessler, R. B. (2000). Connexin 40, bundle-branch block, and propagation at the Purkinje-myocyte junction. *Circ. Res.* **87**, 835-836.

Sedmera, D., Reckova, M., De Almeida, A., Coppen, S. R., Kubalak, S. W., Gourdie, R. G. and Thompson, R. P. (2003). Spatiotemporal pattern of commitment to slowed proliferation in the embryonic mouse heart indicates progressive differentiation of the cardiac conduction system. *Anat. Rec.* **274A**, 773-777.

Sibony, M., Commo, F., Callard, P. and Gasc, J. M. (1995). Enhancement of mRNA in situ hybridization signal by microwave heating. *Lab. Invest.* **73**, 586-591.

Simon, A. M., Goodenough, D. A. and Paul, D. L. (1998). Mice lacking connexin40 have cardiac conduction abnormalities characteristic of atrioventricular block and bundle branch block. *Curr. Biol.* **8**, 295-298.

Surawicz, B. and Knilans, T. K. (2001a). *Chou's Electrocardiography in Clinical Practice: Adult and Pediatric*, 5th edn, p. 11. Philadelphia, PA: W. B. Saunders.

Surawicz, B. and Knilans, T. K. (2001b). Chou's Electrocardiography in Clinical Practice: Adult and Pediatric. 5th edn, pp. 75-76, 93-94. Philadelphia, PA: W. B. Saunders.

Tamaddon, H. S., Vaidya, D., Simon, A. M., Paul, D. L., Jalife, J. and Morley, G. E. (2000). High-resolution optical mapping of the right bundle branch in connexin40 knockout mice reveals slow conduction in the specialized conduction system. *Circ. Res.* **87**, 929–936.

van Rijen, H. V., van Veen, T. A., van Kempen, M. J., Wilms-Schopman, F. J., Potse, M., Krueger, O., Willecke, K., Opthof, T., Jongsma, H. J. and de Bakker, J. M. (2001). Impaired conduction in the bundle branches of mouse hearts lacking the gap junction protein connexin40. *Circulation* **103**, 1591-1598.

Wenink, A. C. (1976). Development of the human cardiac conduction system. *J. Anat.* **121**, 617-631.

Wessels, A., Vermeulen, J. L., Verbeek, F. J., Viragh, S., Kalman, F., Lamers, W. H. and Moorman, A. F. (1992). Spatial distribution of 'tissue-specific' antigens in the developing human heart and skeletal muscle. III. An immunohistochemical analysis of the distribution of the neural tissue antigen G1N2 in the embryonic heart; implications for the development of the atrioventricular conduction system. *Anat. Rec.* **232**, 97-111.